Differential cross section analysis for electron–hydrogen molecule collisions across various energies

Cite as: AIP Advances 15, 105203 (2025); doi: 10.1063/5.0284391
Submitted: 14 June 2025 • Accepted: 18 September 2025 •
Published Online: 2 October 2025

Ahlam Yassir,[1,a] Aqeel Hussain,[1,b] Ahmed Abdullah,[2,c] and Falhy Ali[3,d]

AFFILIATIONS

[1] Department of Physics, College of Sciences, University of Basrah, Basrah, Iraq
[2] Al-Manara College for Medical Sciences, Misan, Iraq
[3] Department of Basic Science, College of Dentistry, Al Maaqal University, Basrah, Iraq

[a] **Author to whom correspondence should be addressed:** ahlam.ashour.sci@uobasrah.edu.iq
[b] Aqeel.hussain@uobasrah.edu.iq
[c] ahmedalsalm@uomanara.edu.iq
[d] Falhy.Ali@almaaqal.edu.iq

ABSTRACT

This work reports comprehensive calculations of differential, elastic, and momentum transfer cross sections, as well as spin polarization, for elastic electron scattering from hydrogen molecules at incident energies of 10, 20, 40, 100, 400, and 700 eV. The analysis is carried out within a relativistic Dirac equation framework using partial-wave expansion and an optical model potential derived from a single-center Hartree–Fock method. The adopted model incorporates numerically evaluated static potentials and systematically accounts for exchange, correlation, and polarization effects through well-established quantum mechanical approximations. The results demonstrate that exchange and polarization interactions play a dominant role at low incident energies and small scattering angles. The calculated differential cross sections show close agreement with a broad set of experimental data reported in the literature. Overall, the study provides reliable relativistic predictions that enhance the understanding of electron–molecule interactions and confirm the robustness of relativistic quantum scattering models, with implications for applications in nuclear physics, atmospheric science, and plasma research.

I. INTRODUCTION

Electron collision physics encompasses a wide range of atomic and molecular processes that are fundamental to understanding matter interactions at the microscopic level. Combining both experimental and theoretical approaches has been essential to advance our knowledge and refine existing models.[1,2]

Elastic scattering of electrons as they traverse matter exerts a significant influence on electron transport phenomena, which are fundamental to numerous scientific and technological applications. Therefore, a comprehensive understanding of differential cross sections (DCSs) for electron scattering is essential for the accurate modeling and prediction of these processes.[3] Electron impact interactions with molecular hydrogen (H_2), particularly dissociative excitation (DE), play a crucial role in diverse environments, including low-temperature plasmas, nuclear fusion devices, planetary atmospheres, and the interstellar medium.[4] These interactions strongly influence the dynamics and chemical composition of such systems and represent essential components in collisional–radiative models.[5] Numerous theoretical models have been developed to describe electron–molecule scattering. Among them, the independent atom model (IAM) offers a simplified framework by approximating molecules as a collection of isolated atoms, which is particularly applicable at higher energies.[6–10] However, more advanced quantum

mechanical methods, such as the Hartree–Fock (HF) approach, enable detailed calculations of molecular wavefunctions and interaction potentials, thereby enhancing the accuracy and reliability of scattering predictions.[11–14] The primary objective of this study is to compute differential, total elastic, and momentum transfer cross sections, along with spin polarization, for elastic electron scattering from hydrogen molecules. These calculations are carried out using a single-center molecular Hartree–Fock method embedded within a relativistic Dirac partial-wave framework. The validity of the theoretical model is assessed by comparing the computed differential and total cross sections (DCS and TCS) with available experimental data.[15,16] Although extensive research has been devoted to electron scattering from molecular hydrogen, significant challenges remain in achieving consistent theoretical predictions that fully incorporate relativistic effects and accurately describe exchange and polarization interactions across a broad range of incident energies.[17] This study addresses these challenges by employing a relativistic Dirac equation framework in combination with a single-center molecular Hartree–Fock optical potential, thereby achieving improved accuracy and providing comprehensive coverage from low to intermediate electron impact energies. The proposed approach is designed to bridge existing gaps between theory and experiment while deepening the understanding of electron–molecule scattering mechanisms.

Furthermore, this work contributes to advancing knowledge of electron–molecule interactions with relevance to diverse fields, including nuclear physics, atmospheric science, and plasma physics. By enhancing the theoretical predictions of scattering parameters, the study supports the development of accurate and reliable models for electron transport in various physical environments.

In this framework, elastic scattering of electrons by molecules is described using a potential model in which the incoming electron (projectile) interacts with the target molecule through an effective potential that represents the total influence of the molecule on the incident electron.

II. OUTLINE OF THE THEORY

The theoretical description of elastic electron scattering from hydrogen molecules in this study is formulated within the framework of the relativistic Dirac equation in combination with an optical model potential. The total interaction potential comprises contributions from the static electrostatic field, exchange effects arising from the indistinguishability of electrons, dynamic polarization of the target, and many-body correlation interactions.[18] This section presents a detailed overview of the components incorporated in the calculation of scattering cross sections.

A. Total interaction potential

The total potential V(r) experienced by the incident electron is expressed as[18]

$$V(r) = V_{st}(r) + V_{ex}(r) + V_{cor}(r) + V_{pol}(r), \quad (1)$$

where $V_{st}(r)$ is the static electrostatic potential, $V_{ex}(r)$ is the exchange potential, $V_{cor}(r)$ is the correlation potential, and $V_{pol}(r)$ is the polarization potential.

This total potential is treated as spherically symmetric using a single-center approximation, suitable for diatomic systems such as H_2.

B. Dirac equation

The relativistic motion of the electron is described by the Dirac equation,[19]

$$[c\alpha \cdot \mathbf{p} + \beta m_0 c^2 + V(r)]\psi(r) = E\psi(r), \quad (2)$$

where c is the speed of light in vacuum, m_0 is the rest mass of the electron, α and β are Dirac matrices, ψ(r) is the wavefunction of the scattered electron, and $E = \gamma m_0 c^2 = E_i + m_0 c^2$ is the total energy, in which $\gamma = (1 - v^2/c^2)^{-1/2}$.

C. Static potential

The static potential $V_{st}(r)$ is derived from the electron charge distribution ρ(r) in the molecule,

$$V_{st}(r) = -\int \frac{\rho(r)'}{|r - r'|} d^3r'. \quad (3)$$

This represents the Coulomb interaction between the incoming electron and the target's charge cloud.

D. Exchange potential

Exchange effects arise from the indistinguishability of electrons. The Furness and McCarthy exchange potential is employed here,[20]

$$V_{ex}^{(-)}(\bar{r}) = \frac{1}{2}[E - V_{st}(\bar{r})] - \frac{1}{2}\left[[E - V_{st}(\bar{r})]^2 + 4\pi a_0 e^4 \rho(r)\right]^{\frac{1}{2}}, \quad (4)$$

where a_0 is the Bohr radius and ρ(r) is the local electron density.

E. Polarization potential

The long-range polarization interaction is modeled by the Buckingham potential,[21]

$$V_{pol}(\bar{r}) = -\frac{\alpha_p e^2}{2\left(r^2 + d^2\right)^2}, \quad (5)$$

where α_p is the molecular polarizability and d is the cutoff parameter to avoid divergence at r = 0. We formulate b_{pol}, adjustable energy-dependent parameter, in terms of Z, atomic number, as follows:

$$b_{pol}^2 = \max\left[\frac{E - 50\ \text{eV}}{16\ \text{eV}}, 1\right]. \quad (6)$$

The cutoff parameter is defined as

$$d^4 = \frac{1}{2}\alpha_p \alpha_0 Z^{-1/3} b_{pol}^2,$$

following Mittleman and Watson.

F. Correlation potential

To account for short-range electron–electron correlations, we adopt the local-density approximation proposed by O'Connell and Lane,[22]

$$2v_c[\rho] \equiv \begin{cases} 0.0622 \ln r_s - 0.096 + 0.018 r_s \ln r_s - 0.02 r_s \\ -0.1231 + 0.037\,96 \ln r_s, \qquad 0.7 < r_s \le 10, \\ -0.876 r_s^{-1} + 2.65 r_s^{-\frac{3}{2}} - 2.8 r_s^{-2} - 0.8 r_s^{-\frac{5}{2}}, \\ 10 \le r_s, \end{cases} \tag{7}$$

where

$$r_s = (3/4\pi\rho)^{\frac{1}{3}}.$$

Although Perdew–Zunger provides an alternative correlation model, O'Connell and Lane's form is chosen here for its balance between computational efficiency and accuracy in low-Z systems, such as H_2.

G. Inelastic channels and optical potential

The imaginary part of the complex optical potential, $-iW_{abs}(r)$, accounts for inelastic scattering channels. This part represents the probability loss due to excitation or ionization,[23–25]

$$\sigma_{inel} = \sigma_{tot} - \sigma_{el}. \tag{8}$$

The **inelastic threshold** is inherently modeled through $W_{abs}(r)$, which becomes significant once the incident energy surpasses the excitation/ionization limits of the target.

H. Partial-wave formalism and cross sections

The scattering amplitude consists of spin-conserving $f(\theta)$ and spin-flip $g(\theta)$ components, derived from phase shifts δ_ℓ,[26–28]

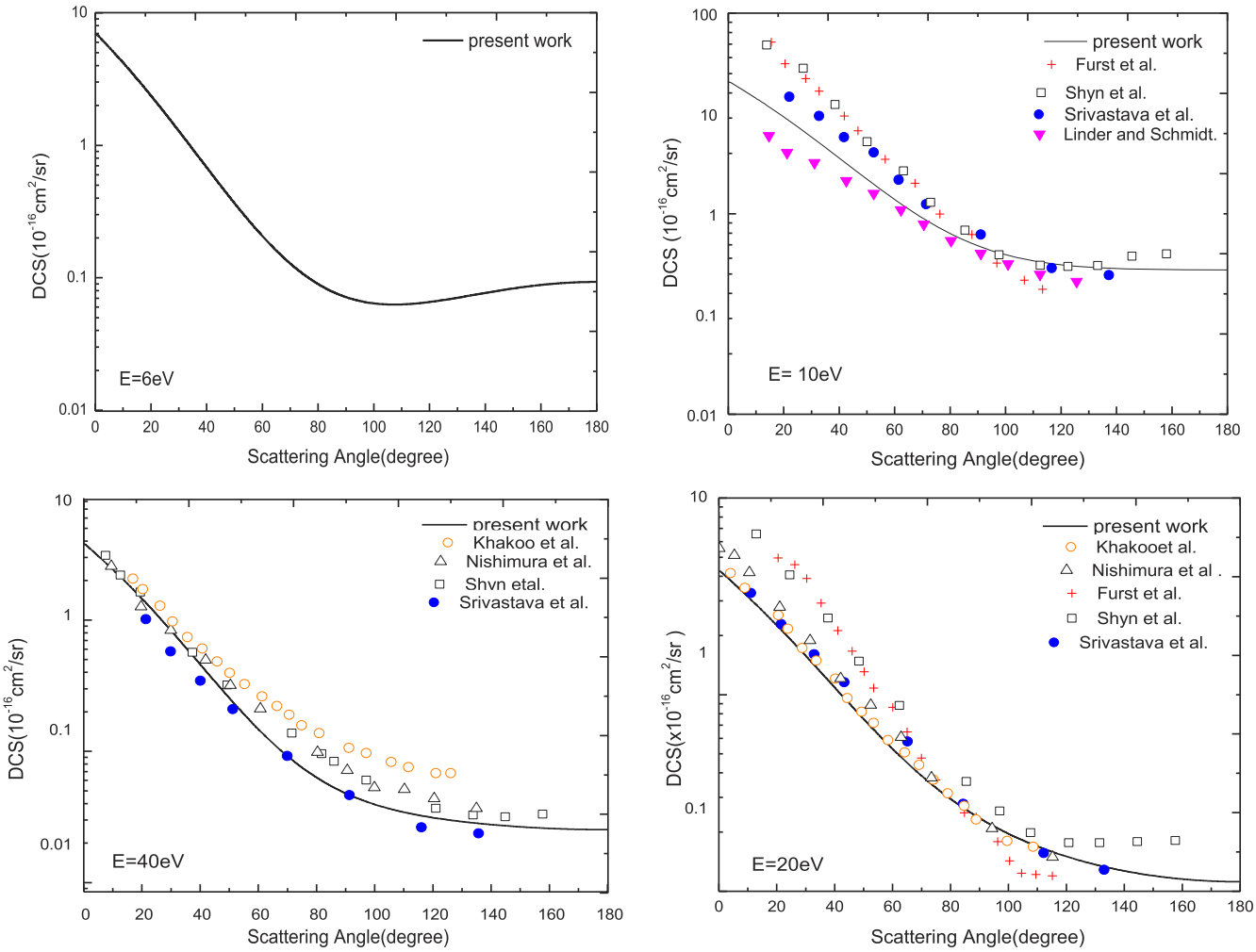

FIG. 1. DCS (10–16 cm^2/sr) for elastic scattering of electrons of hydrogen at energies of 6, 10, 20, and 40 eV. Experimental: Furst *et al.*,[30] Shyn and Sharp,[14] Srivastava *et al.*,[31] Linder and Schmidt,[32] Khakoo *et al.*,[33] Nishimura *et al.*,[34] and Mittleman and Watson.[21]

$$f(\theta) = \frac{1}{2ik}\sum_{\ell=0}^{\infty}\{(\ell+1)[\exp(2i\delta_{\kappa=-\ell-1}) - 1] + \ell[\exp(2i\delta_{K=\ell}) - 1]\}P_\ell(\cos(\theta)), \quad (9)$$

$$g(\theta) = \frac{1}{2ik}\sum_{\ell=0}^{\infty}[\exp(2i\delta_{\kappa=\ell}) - \exp(2i\delta_{K=-\ell-1})]P_\ell^1(\cos\theta). \quad (10)$$

The differential cross section (DCS) is given by

$$\frac{d\sigma}{d\Omega} = |f(\theta)|^2 + |g(\theta)|^2. \quad (11)$$

The total elastic and momentum transfer cross sections are

$$\sigma_{el} = \int \frac{d\sigma}{d\Omega}d\Omega = 2\pi\int_0^{\pi}\left(\frac{d\sigma}{d\Omega}\right)\sin(\theta)d\theta, \quad (12)$$

$$\sigma_m = 2\pi\int_0^{\pi}(1-\cos\theta)\left(\frac{d\sigma}{d\Omega}\right)\sin(\theta)d\theta, \quad (13)$$

where k is the electron wave number, $\delta_{=\pm\ell}$ are phase shifts for spin-up/spin-down channels, P_ℓ is the Legendre polynomial, and ${}^1_\ell P$ is the associated Legendre function.

I. Screening correction (si-correction)

At higher energies, the interference between atomic centers and multiple scattering effects becomes non-negligible. To compensate, the si-correction factor sis_isi introduced by Blanco is applied,[28,29]

$$\varepsilon_i^{(m)} = \frac{N-m+1}{N-1}\sum_{i\neq j}\frac{\sigma_{j\varepsilon_i(m-1)}}{\alpha_{ij}} \quad (m = 2,\ldots,N), \quad (14)$$

where N is the number of atoms in the molecule, α_{ij} is the effective overlap parameter between atoms i and j, and σ_j is the total cross section of atom j.

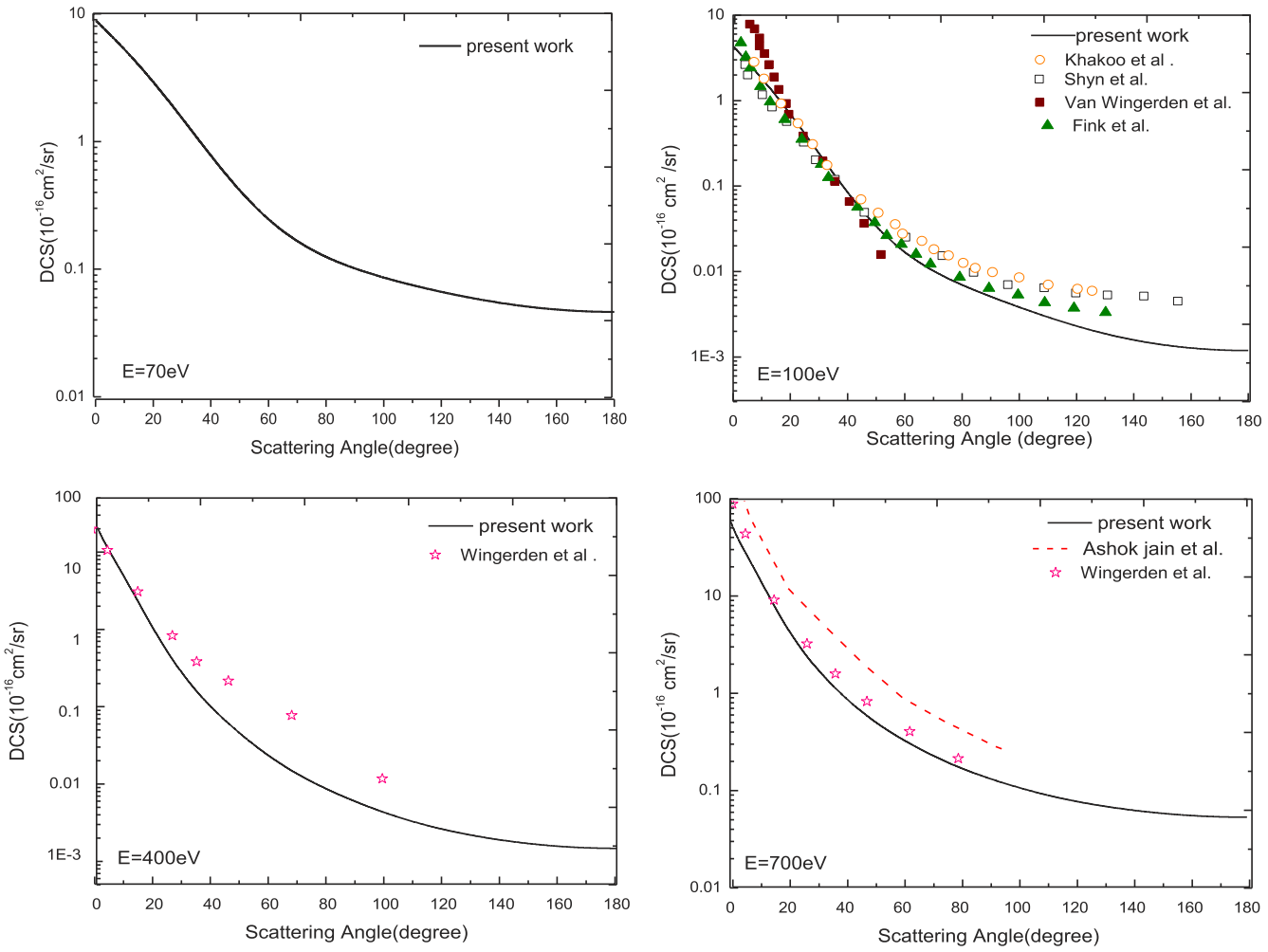

FIG. 2. DCS (10^{-16} cm^2/sr) for elastic scattering of electrons of hydrogen at energies of 70, 100, 400, and 700 eV. Theoretical: Ashok *et al.*[35] Experimental: Wingerden *et al.*[36] and Haque *et al.*[27]

This correction improves accuracy by addressing multiple scattering paths and coherent contributions in molecular systems.

III. RESULTS AND DISCUSSION

Using the optical model potential, we perform relativistic calculations of the total cross section (TCS), differential cross section (DCS), and momentum transfer cross section (MTCS) for electron collisions with H_2 molecules at incident energies of 10, 20, 40, 100, 400, and 700 eV. The calculations incorporate both the real and imaginary components of the potential to consistently account for elastic and inelastic scattering processes.

Figure 1 illustrates the differential cross section (DCS) for electron–H_2 collisions at 10 eV, together with experimental data reported in previous studies for comparison: Furst *et al.*, Shyn and Sharp, Srivastava *et al.*, and Linder *et al.* For 20 eV, the results are compared with data from Khakoo *et al.*, Nishimura *et al.*, Furst *et al.*, Shyn and Sharp, and Srivastava *et al.* For 40 eV, comparisons are made with Refs. 14, 31, 33, and 34, and for 100 eV, the outcomes are evaluated against Refs. 14, 27, 33, and 36.

Figure 2 shows the obtained DCS at 400 eV, compared with experimental data[36] and theoretical results from Ref. 35.

Figure 3 presents the results of the total cross section (TCS) and momentum transfer cross section (MTCS). The TCS data are compared with both experimental measurements and theoretical predictions available in the literature from Shyn and Sharp[14] and Srivastava *et al.*,[31] while the MTCS values are validated against theoretical predictions by England *et al.*[39] and empirical data from Refs. 14, 36, and 37.

Figure 4 illustrates the behavior of Sherman's function, showing strong spin polarization effects at low energies (6, 10, 20, 40, 70, and 100 eV) due to quantum interference, with oscillations that gradually diminish at higher energies (400 and 700 eV), indicating a transition toward classical behavior.

At high incident energies, the interference structures arising from quantum wave interactions gradually diminish. As illustrated in Fig. 4, a distinct transition is observed from pronounced spin polarization effects—characterized by oscillatory features of Sherman's function at low energies (6, 10, 20, 40, 70, and 100 eV) to a more classical scattering behavior at higher energies (400 and 700 eV), where the oscillations in Sherman's function are significantly suppressed. This trend reflects the reduced influence of quantum interference and spin-dependent effects with increasing electron energy.

At higher collision energies, the electron–molecule interaction tends to localize within the inner electronic shells (e.g., the K-shell). In this regime, scattered waves originating from different directions interfere incoherently, leading to the disappearance of interference patterns. This observation is consistent with the DCS results shown in Figs. 1–3, where the de Broglie wavelength of the incident electron becomes much smaller than the interatomic separations within the H_2 molecule. Consequently, the incoming electrons interact independently with each constituent atom, thereby minimizing geometrical overlap effects.

Although H_2 is one of the most fundamental molecules in physics and chemistry, theoretical investigations of its electron–collision dynamics remain relatively limited because of the inherent complexity of modeling quantum interactions. Much of the previous research has concentrated on experimental measurements. The present study contributes by providing reliable and up-to-date theoretical predictions that closely reproduce available empirical data, thereby validating the effectiveness of the applied relativistic optical model. These findings offer valuable insights for refining collision dynamics models and support future advances in fields such as nuclear physics, plasma research, and molecular electronics.

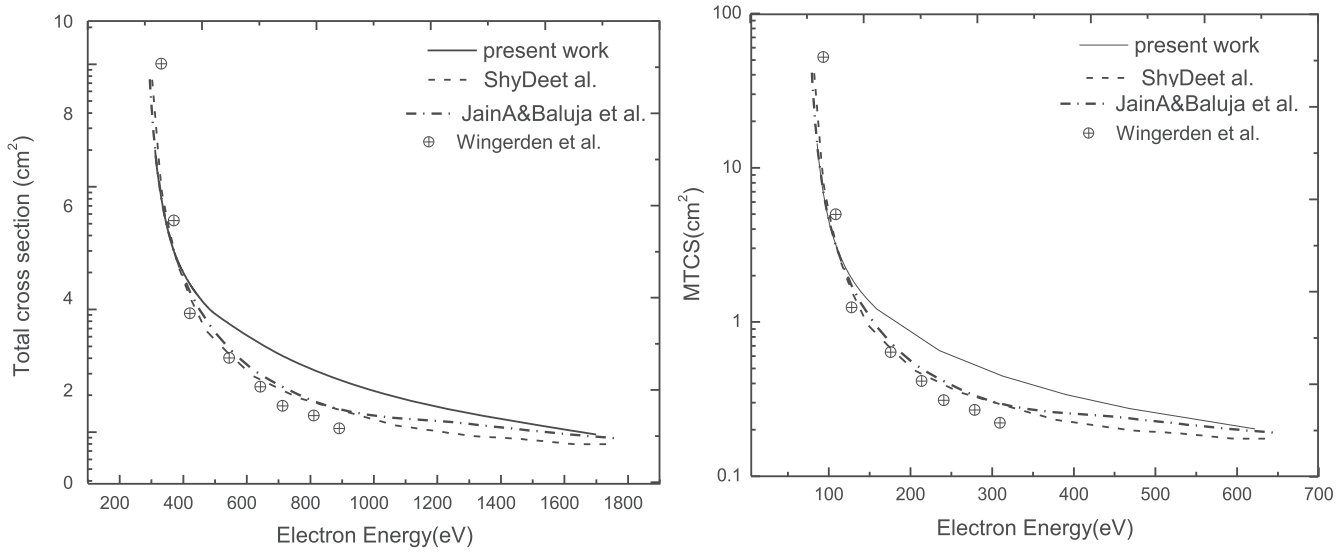

FIG. 3. TCS (left) and MTCS (right) for the elastic scattering of electrons from H_2. Theoretical: Jain and Baluja,[37] De-Heng *et al.*,[38] Wingerden *et al.*,[36] and England *et al.*[39] Experimental: Nishimura *et al.*[34] and Shyn and Sharp.[14]

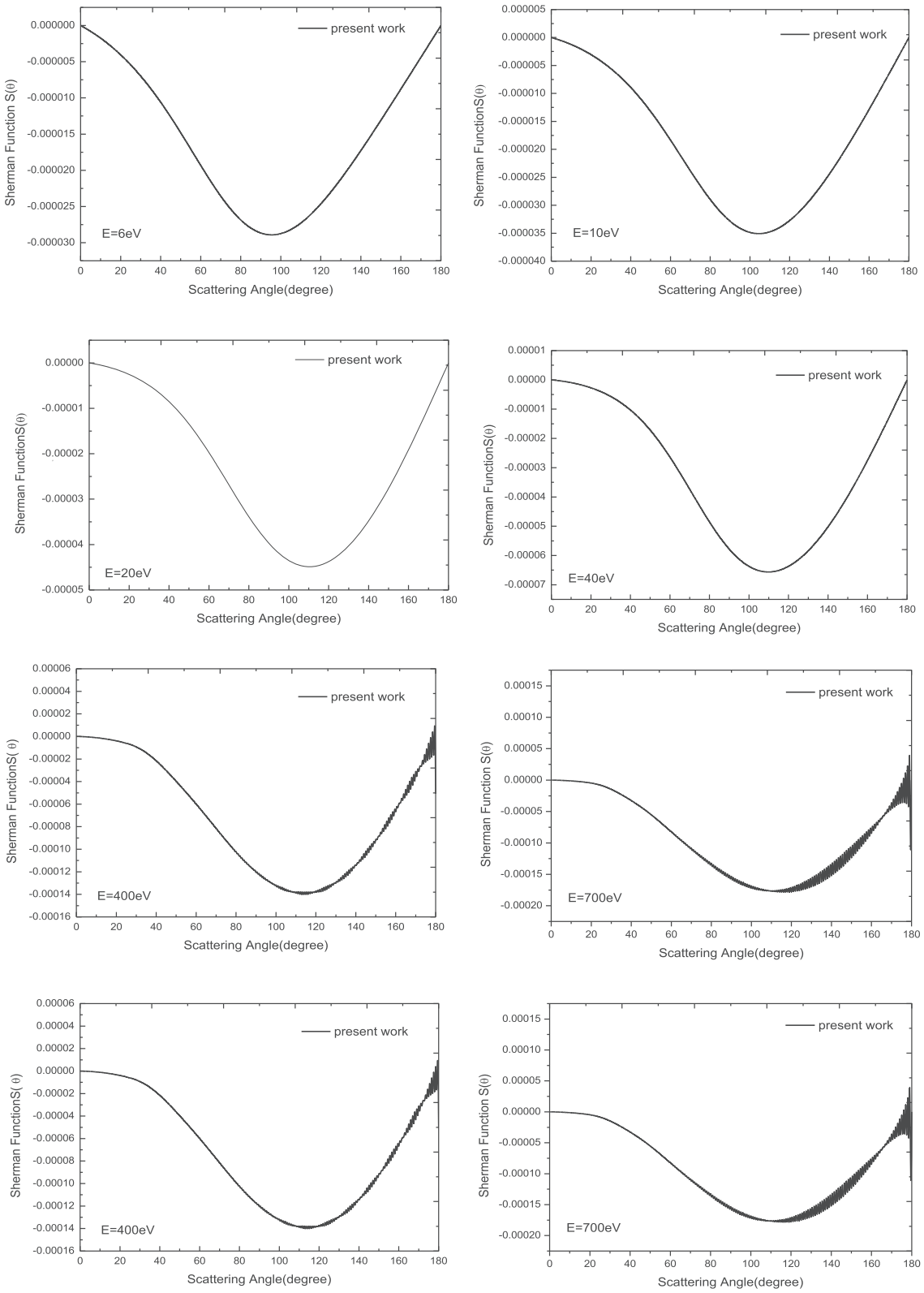

FIG. 4. The Sherman function describes spin polarization at collision with a hydrogen molecule at the following energies: 6, 10, 20, 40, 70, 100, 400, and 700 eV.

The interference structures observed in the DCS are primarily attributed to diffraction effects that arise at low incident energies as a consequence of the wave-like nature of electrons. These structures are strongly dependent on scattering angle and energy, thereby revealing detailed information about the molecular potential landscape. With increasing energy, such structures gradually disappear, and incoherent scattering becomes dominant due to the diminished significance of wave-like behavior.

Moreover, the overall decrease observed in the TCS, DCS, and MTCS values with increasing incident energy can be attributed to several underlying factors, which are as follows:

1. **Nature of interactions**: At low energies, elastic scattering dominates, whereas at higher energies, additional inelastic channels become accessible, thereby reducing the elastic contribution and lowering the total cross section.
2. **Quantum interference**: At specific energies, quantum interference effects may either enhance or suppress scattering probabilities. As the energy increases, these quantum effects gradually diminish, leading to smoother trends and lower cross section values.
3. **Scattering angle dependence**: Larger scattering angles generally correspond to lower DCS values due to the reduced probability of forward scattering. Angular variations can, therefore, significantly influence the overall shape of the DCS curve.
4. **Momentum transfer**: Increasing projectile momentum shortens the interaction time and decreases the likelihood of effective scattering, thereby contributing to the gradual decline in cross section values. Finally, although thermal effects can influence cross sections in plasma environments, they are not explicitly incorporated in the present theoretical model and are thus not considered in this study.

IV. CONCLUSIONS

The differential and total cross sections (DCS and TCS) were calculated using the relativistic Dirac equation with partial-wave analysis. The results show good agreement with both theoretical predictions and available experimental measurements, particularly at medium and high energies.

The DCS values exhibit a pronounced energy dependence, being relatively higher at lower incident energies (6–20 eV), which reflects an increased probability of interaction with hydrogen molecules. With increasing energy, the DCS decreases, consistent with theoretical expectations due to the shorter de Broglie wavelength of the incident electrons.

The TCS systematically decreases over the energy range of 10–700 eV. This trend can be explained by the combined influence of elastic and inelastic scattering channels. Similarly, the momentum transfer cross section declines at higher energies, indicating the reduced contribution of low-energy states in high-energy collisions.

The Sherman function reveals strong oscillatory behavior at low energies, signifying that spin polarization effects appear due to wave interference at low energies. These oscillations are markedly suppressed at higher energies, indicating a transition from quantum interference phenomena to more classical scattering behavior.

In conclusion, this study highlights the strong dependence of molecular scattering characteristics, with quantum effects such as spin polarization dominating at low incident energies, while classical features prevail at higher energies. These findings provide valuable insights into electron–molecule scattering dynamics and contribute to the development of more accurate theoretical models.

AUTHOR DECLARATIONS

Conflict of Interest

The authors have no conflicts to disclose.

Author Contributions

Ahlam Yassir: Writing – original draft (equal). **Aqeel Hussain**: Resources (equal); Software (equal). **Ahmed Abdullah**: Resources (equal); Writing – review & editing (equal). **Falhy Ali**: Supervision (equal).

DATA AVAILABILITY

The data that support the findings of this study are available within the article.

REFERENCES

[1] B. C. Saha *et al.*, "Elastic scattering of electrons and positrons from alkali atoms," Adv. Quantum Chem. **86**, 1–149 (2022).
[2] A. K. Yassir, "Differential cross-section elastic scattering of electrons by silver atoms," Basrah J. Sci. **40**(2), 389–399 (2022).
[3] M. H. Khandker, A. K. F. Haque, M. M. Haque, M. M. Billah, H. Watabe, and M. A. Uddin, "Relativistic study on the scattering of $e^{\pm}$ from atoms and ions of the Rn isonuclear series," Atoms **9**(3), 59 (2021).
[4] R. M. Abdul Hassan and A. A. Khalaf, "Atomic lithium excitation by electron impact," J. Kufa-Phys. **11**(02), 29–33 (2019).
[5] D. Belkic, *Principles of Quantum Scattering Theory* (CRC Press, 2020).
[6] T. L. Stephens and A. Dalgarno, "Spontaneous radiative dissociation in molecular hydrogen," J. Quant. Spectrosc. Radiat. Transfer **12**(4), 569–586 (1972).
[7] H. Abgrall, E. Roueff, X. Liu, and D. E. Shemansky, "The emission continuum of electron-excited molecular hydrogen," Astrophys. J. **481**(1), 557 (1997).
[8] H. Melin, D. E. Shemansky, and X. Liu, "The distribution of atomic hydrogen and oxygen in the magnetosphere of Saturn," Planet. Space Sci. **57**(14-15), 1743–1753 (2009).
[9] D. E. Shemansky, X. Liu, and H. Melin, "The Saturn hydrogen plume," Planet. Space Sci. **57**(14-15), 1659–1670 (2009).
[10] V. A. Shakhatov and Y. A. Lebedev, "Kinetics of populations of singlet and triplet states in non-equilibrium hydrogen plasma," J. Phys. D: Appl. Phys. **51**(21), 213001 (2018).
[11] K. Sawada and M. Goto, "Rovibrationally resolved time-dependent collisional-radiative model of molecular hydrogen and its application to a fusion detached plasma," Atoms **4**(4), 29 (2016).
[12] A. K. Yassir, A. H. Hussain, and F. A. Ali, J. Kufa Phys. **13**, 1 (2021).
[13] R. J. Bartlett and J. F. Stanton, "Applications of post-Hartree–Fock methods: A tutorial," Rev. Comput. Chem. **5**, 65–169 (1994).
[14] T. W. Shyn and W. E. Sharp, "Angular distributions of electrons elastically scattered from H_2," Phys. Rev. A **24**(4), 1734 (1981).
[15] A. K. Yassir and A. A. Khalaf, "Rotational excitation of methane molecule by electron impact," Int. J. Chem. Math. Phys. **8**(3), 1 (2024).
[16] D. Das, "Probing fundamental aspects of spatial and temporal quantum correlations," Ph.D. thesis (2019), https://doi.org/10.13140/RG.2.2.12791.65447.
[17] A. F. Goncharov, "Simple molecules at high pressures: Transitions to extended and atomic states," High-Pressure Mol. Spectrosc. **9**, 91 (2022).

[18]F. Salvat, A. Jablonski, and C. J. Powell, "ELSEPA—Dirac partial-wave calculation of elastic scattering of electrons and positrons by atoms, positive ions and molecules," Comput. Phys. Commun. **165**(2), 157–190 (2005).
[19]P. A. M. Dirac, *The Principles of Quantum Mechanics* (Oxford University Press, 1981), Vol. 27.
[20]M. N. A. Abdullah, A. Kumar, A. K. F. Haque, and M. Alfaz Uddin, "A study of critical minima and spin polarization in the $e^{\pm}$–Ba elastic scattering," Eur. Phys. J. D **74**(12), 235 (2020).
[21]M. H. Mittleman and K. M. Watson, "Effects of the Pauli principle on the scattering of high-energy electrons by atoms," Ann. Phys. **10**(2), 268–279 (1960).
[22]J. K. O'Connell and N. F. Lane, "Nonadjustable exchange-correlation model for electron scattering from closed-shell atoms and molecules," Phys. Rev. A **27**(4), 1893 (1983).
[23]F. Salvat, "Optical-model potential for electron and positron elastic scattering by atoms," Phys. Rev. A **68**(1), 012708 (2003).
[24]R. Hassan *et al.*, "Scattering of $e^{\pm}$ off silver atom over the energy range 1 eV–1 MeV," Eur. Phys. J. D **75**(7), 204 (2021).
[25]A. Abdullah and A. H. Hussain, "Critical positions and spin polarisation for electrons scattered by potassium atoms," Mol. Phys. **122**(13), e2300323 (2024).
[26]M. Ismail Hossain, A. K. F. Haque, M. Atiqur, R. Patoary, M. A. Uddin, and A. K. Basak, "Elastic scattering of electrons and positrons by atomic magnesium," Eur. Phys. J. D **70**(2), 41 (2016).
[27]A. K. F. Haque *et al.*, "A study of the critical minima and spin polarization in the elastic electron scattering by the lead atom," J. Phys. Commun. **2**(12), 125013 (2018).
[28]A. K. Yassir and A. A. Khalaf, "Electron collision with ammonia and phosphine at wide range of energies," J. Kufa-Phys. **14**(02), 59–74 (2022).
[29]F. Blanco, L. Ellis-Gibbings, and G. García, "Screening corrections for the interference contributions to the electron and positron scattering cross sections from polyatomic molecules," Chem. Phys. Lett. **645**, 71–75 (2016).
[30]J. Furst, M. Mahgerefteh, and D. E. Golden, "Absolute total electronically elastic differential e^{-}-H_2 scattering cross-section measurements from 1 to 19 eV," Phys. Rev. A **30**(5), 2256 (1984).
[31]S. K. Srivastava, A. Chutjian, and S. Trajmar, "Absolute elastic differential electron scattering cross sections in the intermediate energy region. I. H_2," J. Chem. Phys. **63**(6), 2659–2665 (1975).
[32]F. Linder and H. Schmidt, "Rotational and vibrational excitation of H_2 by slow electron impact," Z. Naturforsch. A **26**(10), 1603–1617 (1971).
[33]M. Khakoo, P. Johnson, I. Ozkay, P. Yan, S. Trajmar, and I. Kanik, "Differential cross sections for the electron impact excitation of the $A\,^3\Sigma_u^+$, $B\,^3\Pi_g$, $W\,^3\Delta_u$, $B'\,^3\Sigma_u^-$, $a'\,^1\Sigma_u^-$, $a\,^1\Pi_g$, $w\,^1\Delta_u$, and $C\,^3\Pi_u$ states of N_2," Phys. Rev. A **71**(6), 062703 (2005).
[34]H. Nishimura, A. Danjo, and H. Sugahara, "Differential cross sections of electron scattering from molecular hydrogen I. Elastic scattering and vibrational excitation ($X^1\Sigma_g^+$, $v = 0 \rightarrow 1$)," J. Phys. Soc. Jpn. **54**(5), 1757–1768 (1985).
[35]S. Ashok, J. M. Borrego, and R. J. Gutmann, "Electrical characteristics of GaAs MIS Schottky diodes," Solid-State Electron. **22**(7), 621–631 (1979).
[36]B. van Wingerden, R. W. Wagenaar, and F. de Heer, "Total cross sections for electron scattering by molecular hydrogen," J. Phys. B: At. Mol. Phys. **13**(17), 3481 (1980).
[37]A. Jain and K. L. Baluja, "Total (elastic plus inelastic) cross sections for electron scattering from diatomic and polyatomic molecules at 10–5000 eV: H_2, Li_2, HF, CH_4, N_2, CO, C_2H_2, HCN, O_2, HCl, H_2S, PH_3, SiH_4, and CO_2," Phys. Rev. A **45**(1), 202 (1992).
[38]S. De-Heng, S. Jin-Feng, Y. Xiang-Dong, Z. Zun-Lue, and L. Yu-Fang, "Total cross sections for scattering of electrons from O_2, H_2O, H_2, O_3, CO and CO_2 at 100–2000 eV," Chin. Phys. **13**(7), 1018 (2004).
[39]J. England, M. Elford, and R. Crompton, "A study of the vibrational excitation of H_2 by measurements of the drift velocity of electrons in H_2–Ne mixtures," Aust. P. Phys. **41**(4), 573–586 (1988).